The Paralogous *Hox* Genes *Hoxa10* and *Hoxd10* Interact to Pattern the Mouse Hindlimb Peripheral Nervous System and Skeleton

George M. Wahba,* Sirkka Liisa Hostikka,† and Ellen M. Carpenter*,[1]

**Mental Retardation Research Center, Department of Psychiatry and Biobehavioral Sciences, UCLA School of Medicine, 760 Westwood Plaza, Los Angeles, California 90024; and †Department of Human Genetics, University of Utah School of Medicine, Salt Lake City, Utah 84112*

The most 5′ mouse *Hoxa* and *Hoxd* genes, which occupy positions 9–13 and which are related to the Drosophila *AbdB* gene, are all active in patterning developing limbs. Inactivation of individual genes produces alterations in skeletal elements of both forelimb and hindlimb; inactivation of some of these genes also alters hindlimb innervation. Simultaneous inactivation of paralogous or nonparalogous *Hoxa* and *Hoxd* genes produces more widespread alterations, suggesting that combinatorial interactions between these genes are required for proper limb patterning. We have examined the effects of simultaneous inactivation of *Hoxa10* and *Hoxd10* on mouse hindlimb skeletal and nervous system development. These paralogous genes are expressed at lumbar and sacral levels of the developing neural tube and surrounding axial mesoderm as well as in developing forelimb and hindlimb buds. Double-mutant animals demonstrated impaired locomotor behavior and altered development of posterior vertebrae and hindlimb skeletal elements. Alterations in hindlimb innervation were also observed, including truncations and deletions of the tibial and peroneal nerves. Animals carrying fewer mutant alleles show similar, but less extreme phenotypes. These observations suggest that *Hoxa10* and *Hoxd10* coordinately regulate skeletal development and innervation of the hindlimb.

***Key Words:* *Hox* genes; mouse; spinal cord; hindlimb; peripheral nerve; skeletogenesis.**

INTRODUCTION

Mammalian *Hox* genes, which are related to the Drosophila homeotic genes, encode transcription factors which are crucial for regional development along the anterior-posterior axis during embryonic development. The mouse genome contains 39 *Hox* genes linked into four clusters, designated *Hoxa, Hoxb, Hoxc,* and *Hoxd,* which are positioned on four separate chromosomes. These four linkage groups are likely to have arisen by two duplications of an ancestral homeotic complex to produce four clusters of *Hox* genes in which individual genes within a cluster have one or more paralogues with highly conserved sequences and overlapping expression domains in the other clusters (reviewed in Rijli and Chambon, 1997). *Hox* genes are expressed in a temporal and spatial order along the embryonic axis which reflects their position within the gene clusters, with 3′ genes expressed earlier and more rostrally than more 5′ genes (Gaunt *et al.,* 1989; Izpisúa-Belmonte *et al.,* 1991). All *Hox* genes are expressed early in development within the neural tube and surrounding axial mesoderm in overlapping broad domains. In addition to their axial expression, the 16 most 5′ genes, which occupy positions 9–13 within the respective complexes and encode *AbdB* class homeodomain proteins (Bürglin, 1994), are also expressed in developing forelimb and hindlimb buds (Haack and Gruss, 1993; Dollé and Duboule, 1989; Dollé *et al.,* 1989).

Inactivation of the *AbdB*-related members of the *Hoxa* and *Hoxd* clusters has demonstrated a clear role for these genes in axial patterning and in limb development. Mutations in the *Hoxa9–11, Hoxa13,* and *Hoxd9–13* genes all produce anterior transformation of the lumbar and sacral vertebrae, with each gene individually affecting subsets of the thoracic, lumbar, and sacral vertebrae (Small and Potter, 1993; Davis and Capecchi, 1994; Rijli *et al.,* 1995; Satokata

[1] To whom correspondence should be addressed at Department of Psychiatry and Biobehavioral Science, UCLA School of Medicine, 48-228 NPI, 760 Westwood Plaza, Los Angeles, CA 90024. Fax: (310) 206-5050. E-mail: ecarpenter@mednet.ucla.edu.

0012-1606/01 $35.00

et al., 1995; Favier *et al.,* 1996; Fromental-Ramain *et al.,* 1996a; Carpenter *et al.,* 1997). In addition, inactivation of these genes also affects patterning of skeletal elements of both the forelimb and hindlimb (Davis and Capecchi, 1996; Favier *et al.,* 1996; Fromental-Ramain *et al.,* 1996b; Carpenter *et al.,* 1997). Some of these genes have also been implicated in patterning the posterior central and peripheral nervous system. Inactivation of *Hoxa10* produces a spinal nerve transformation (Rijli *et al.,* 1995) while inactivation of *Hoxd10* produces an anterior transformation of the L3 spinal segment and alters peripheral nerve projections into the developing hindlimb (Carpenter *et al.,* 1997). Simultaneous inactivation of paralogous or nonparalogous *Hoxa* and *Hoxd* genes illustrates functional cooperation between these genes by unmasking phenotypes not apparent following single gene inactivation. Inactivation of the paralogous genes *Hoxa9* and *Hoxd9* produced more extensive vertebral and limb transformations (Fromental-Ramain *et al.,* 1996a), inactivation of *Hoxa11* and *Hoxd11* deletes most of the radius and ulna (Davis *et al.,* 1995), and loss of *Hoxa13* and *Hoxd13* eliminates distal cartilage condensation and formation of the autopod (Fromental-Ramain *et al.,* 1996b). Similar cooperation can occur between nonparalogous genes as well, as inactivation of *Hoxa10* and *Hoxd11* produces phenotypes not evident in either single mutant alone (Favier *et al.,* 1996).

We have examined the phenotypic consequences of dual inactivation of *Hoxa10* and *Hoxd10*. Both of these genes are expressed at lumbar levels in the developing neural tube and surrounding mesoderm, as well as in the forelimb and hindlimb. Inactivation of either of these genes alone produces anterior transformation of lumbar vertebrae and alteration in spinal segmental identity (Rijli *et al.,* 1995; Satokata *et al.,* 1995; Carpenter *et al.,* 1997). Single gene inactivation also affects hindlimb development, with *Hoxa10* affecting the femur and both genes independently affecting the knee. Animals carrying mutations in both *Hoxa10* and *Hoxd10* show significant behavioral alterations primarily affecting the hindlimb, as well as morphological alterations in the hindlimb skeleton and peripheral nerves. Our observations suggest both independent activity and functional cooperation between these two genes to pattern skeletal and nervous system elements of the developing hindlimb.

METHODS AND MATERIALS

Generation of Double-Mutant Animals

Hoxa10$^{+/-}$/*Hoxd10*$^{+/-}$ dual heterozygous mice were obtained by crossing *Hoxd10*$^{-/-}$ females with *Hoxa10*$^{+/-}$ males (kindly provided by J. Delort and M. R. Capecchi). Fifty percent of offspring from these crosses were heterozygous at both loci; both male and female dual heterozygous mice appeared behaviorally normal and exhibited normal fertility. *Hoxa10*$^{-/-}$/*Hoxd10*$^{-/-}$ embryos and adult animals were obtained by intercrossing *Hoxa10*$^{+/-}$/*Hoxd10*$^{+/-}$ parents; embryos and adult animals of all expected genotypes were obtained from these intercrosses. Animals were genotyped by extracting DNA as described (Carpenter *et al.,* 1997) from tail biopsies or yolk sacs for adults and embryos, respectively. Samples were subjected to two separate PCR to detect mutations at both loci. *Hoxd10* PCR was performed as previously described (Carpenter *et al.,* 1997), but using the following forward and reverse primers: *Hoxd10* forward, 5′-GAA GAG GTG CCC TTA CAC CA-3′; *Hoxd10* reverse, 5′-TCG ATT CTC TCG GCT CAT CT-3′; KT3NP4 reverse 1, 5′-TTC AAG CCC AAG CTT TCG CGA G-3′. These primers amplify a wild-type band of 182 bp, corresponding to bp 2535–2717 (Renucci *et al.,* 1992), and a mutant band of 139 bp overlapping the KT3NP4 cassette insertion site into the *Hpa*I site of exon 2. *Hoxa10* PCR was performed using the following primers: *Hoxa10* forward, 5′-ATG CAG CCA ACT GGC TCA CAG C-3′; *Hoxa10* reverse, 5′-CTC CGG CAC AGG TGT GAG TTC-3′; KT3NP4 reverse 2, 5′-GGT TGT TCA GAC TAC AAT CTG ACC-3′. PCR cycle conditions were 95°C for 30 s + 2 s/cycle, 59°C for 15 s, 72°C for 45 s for 32 cycles followed by a 7-min terminal extension at 72°C. These reaction conditions amplified a wild-type band of 349 bp, corresponding to bp 1000–1349 of Bensen *et al.* (1995) and a mutant band of 220 bp overlapping the KT3NP4 *neo* cassette insertion site into an *Xho*I restriction site in the homeodomain. Amplified DNA was separated on 1.5% Trevigel agarose gels and visualized by staining with ethidium bromide.

Behavioral Analysis

Locomotor behavior was examined in adult animals by scoring for motility in a modified open-field paradigm as previously described (de la Cruz *et al.,* 1999). Each animal was tested three times with minimum delay of 24 h between trials. One double mutant animal did not complete its third trial. Scores from animals of the same genotype were pooled and used to determine the average number of quadrants entered; pooled values were also subjected to *t* test comparisons between animals of different genotypes and to ANOVA analysis of the overall distribution. Alterations in gait and adduction were identified and scored as previously described (Carpenter *et al.,* 1997).

Skeletal Analysis

Skeletons were prepared from 8-week old mice derived from *Hoxa10*$^{+/-}$/*Hoxd10*$^{+/-}$ intercrosses and examined as described (Mansour *et al.,* 1993). Skeletons were observed for structural alterations in the vertebral column and in the hindlimb. Forelimb skeletal defects were also observed and will be described elsewhere.

Whole-mount Immunohistochemistry Using Antineurofilament

Embryos were collected at E12.5 or E13.5, fixed, eviscerated, and labeled in whole mount using 2H3 monoclonal antibody (Developmental Studies Hybridoma Bank) as previously described (Carpenter *et al.,* 1997; de la Cruz *et al.,* 1999) with minor modification. 2H3 supernatant was used at a dilution of 1:100 in PBSTMD (1% Tween 20, 2% skim milk powder, 1% dimethyl sulfoxide in PBS); embryos were incubated in primary antibody for 3 to 5 days. Embryos were transected, mounted, visualized, and photographed as described (de la Cruz *et al.,* 1999). Nerve position and trajectories were identified using low-power microscopy; individual limbs were photographed in several different planes to reveal the full extent of hindlimb innervation. Nerves were measured from sets of photographs of different limbs taken at the same magnification. Individual nerves were measured only in those limbs where the entire

TABLE 1

Axial Skeletal Phenotypes and Pelvic Position Following *Hoxa10*$^{+/-}$/*Hoxd10*$^{+/-}$ Intercrosses

	Genotype				
Hoxa10	−/−	+/+	−/−	+/−	−/−
Vertebral pattern *Hoxd10*	+/+	−/−	+/−	−/−	−/−
T14L6(L7/S1*)S3[a]					25
T14L6(L7/S1*)S2(S4/C1*)			5.6		
T14L6S4	5.6		11.1	6.7	25
T14L6S3					18.8
T14L5(L6/S1*)S3(S4/C1*)			5.6		
T14L5S4	5.6		11.1		
T13(T14*)L6S4				6.7	6.3
T13(T14*)L6S3			11.1		12.5
T13(T14*)L5(L6/S1*)S4				6.7	
T13(T14*)L5S4	72.3		16.7		12.5
T13L7S4				6.7	
T13L7S3			5.6	6.7	
T13L6(L7/S1*)S4			5.6		
T13L6(L7/S1*)S3				13.3	
T13L6S4	**11.1**	**100**	**22.2**	**46.7**	
T13L6S3			5.6	6.7	
T13L5S4	5.6				
Number of animals analyzed:	18	11	18	15	16

	Genotype								
Hoxa10	+/+	+/−	+/+	+/−	−/−	+/+	−/−	+/−	−/−
Pelvic position[b] *Hoxd10*	+/+	+/+	+/−	+/−	+/+	−/−	+/−	−/−	−/−
L5-C1					11.1		5.6		
L5-S4							5.6		
L6-C1	88.9	12.5	100	50	50		50	33.3	50
L6-C2	11.1	87.5		50	33.3	100	38.9	60	31.3
L6-C3					5.6				6.3
S1-C2								6.7	12.5
Number of animals:	9	8	1	10	18	11	18	15	16

[a] Percentage of animals exhibiting different patterns of thoracic (T), lumbar (L), sacral (S), and caudal (C) vertebrae following *Hoxa10*$^{+/-}$/*Hoxd10*$^{+/-}$ intercrosses. The T13L6S4 pattern indicated in bold predominates in wild-type, single heterozygous, and dual heterozygous animals. Transitional vertebrae, which exhibit features of two classes of vertebrae, are indicated with asterisks.

[b] Percentage of animals derived from *Hoxa10*$^{+/-}$/*Hoxd10*$^{+/-}$ intercrosses exhibiting alterations in pelvic position.

extent of the variable to be measured could be traced and identified. Nerves which lacked distal nerve expansions or branches were scored as 0 μm. For statistical analysis, each limb was treated individually, allowing a single embryo to contribute up to two limbs for analysis.

Statistical Analysis

Nerve measurements were pooled together into groups of nerves measured in animals with the same genotype. Statistical comparisons between groups were made using Student's two-sample *t* tests assuming unequal variances. In addition, ANOVA analysis of all measurements of the same variable was also performed to determine if variations across the entire sample population were significant.

RESULTS

Viability and Behavior of Double Mutants

Hoxa10/Hoxd10 double mutants are viable embryonically and to weaning and adulthood. Following intercrosses of dual heterozygous parents (*Hoxa10*$^{+/-}$/*Hoxd10*$^{+/-}$) embryos and postnatal offspring were produced in a range of genotypes spanning wild-type to double-mutant; double-mutant embryos and adults were produced with approximately the expected frequency assuming Mendelian segregation of alleles. Morphological and behavioral phenotypes of *Hoxa10* and *Hoxd10* single-mutant animals have been previously described (Carpenter *et al.*, 1997; Rijli *et al.*, 1995; Satokata *et al.*, 1995; Favier *et al.*, 1996). Dual

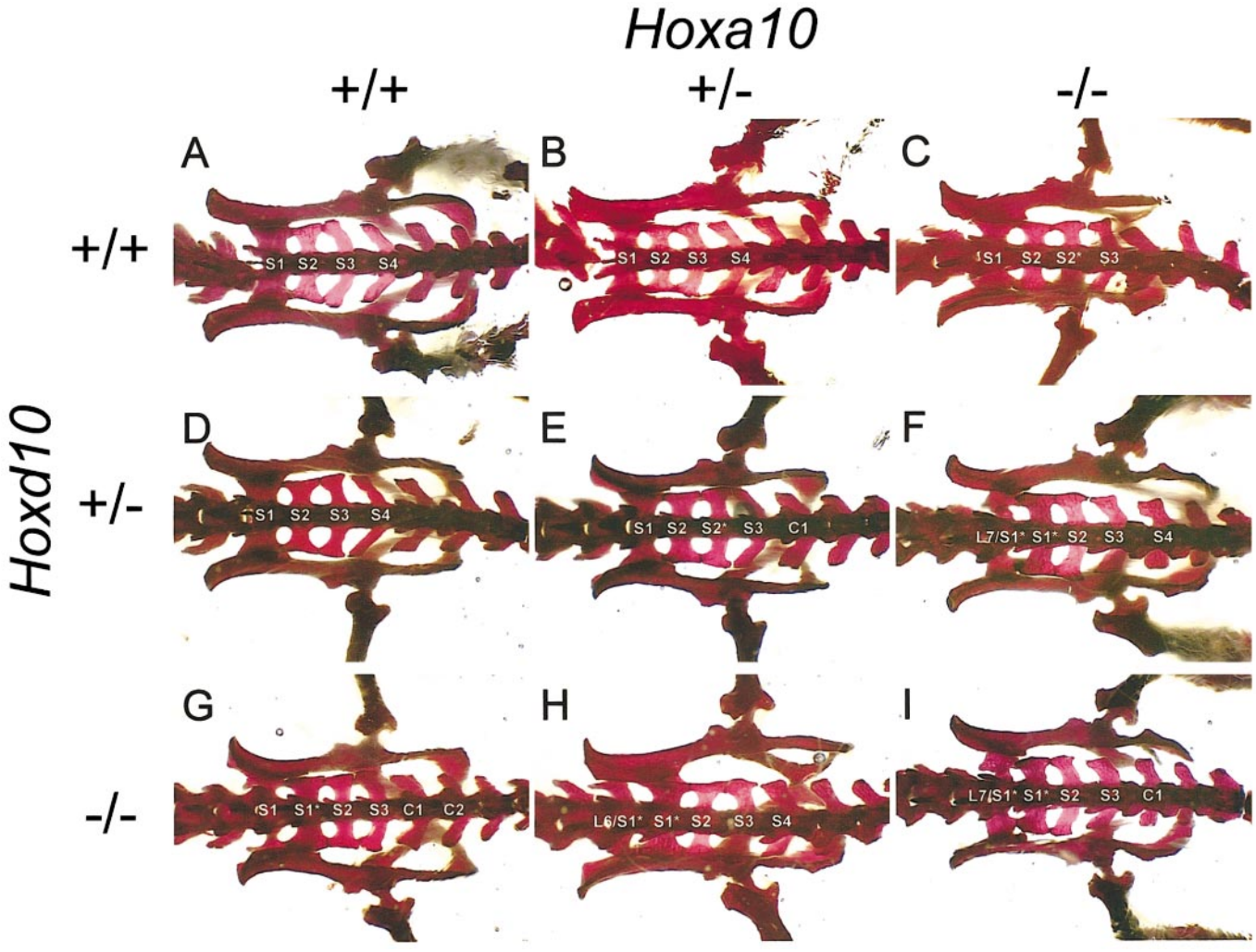

FIG. 1. Sacral vertebrae demonstrate anterior transformation in animals derived from *Hoxa10*$^{+/-}$/*Hoxd10*$^{+/-}$ intercrosses. Animals of all possible genotypes derived from this cross are illustrated in this figure, with *Hoxa10* genotypes distributed left to right and *Hoxd10* genotypes distributed top to bottom. Vertebral identities are indicated on each panel, with transformed vertebrae designated with an asterisk. Wild-type (A) and single heterozygous (B, D), and animals all have four sacral vertebrae (S1–S4). Dual heterozygous animals (E) also have four sacral vertebrae, some of which adopt more anterior morphologies (S2*). The first caudal vertebra is designated C1. *Hoxa10*$^{-/-}$ (C) and *Hoxd10*$^{-/-}$ (G) animals also have sacral vertebrae with more anterior morphologies (S1*, S2*). *Hoxa10*$^{-/-}$/*Hoxd10*$^{+/-}$ (F), *Hoxa10*$^{+/-}$/*Hoxd10*$^{-/-}$ (H), and double-mutant (I) animals have anteriorly transformed sacral vertebrae (S1*) as well as lumbar-sacral transitional vertebrae (L7/S1*, L6/S1*), which have characteristics of two classes of vertebrae.

heterozygous animals appeared phenotypically normal, but significant behavioral alterations were observed in animals carrying three or four mutant alleles. In general, gait abnormalities in animals carrying three mutant alleles resembled gait alterations observed in *Hoxd10*$^{-/-}$ animals (Carpenter *et al.*, 1997), but appeared with greater penetrance and somewhat increased severity. Locomotor behavior in these animals varied from mild stiffness and odd foot position to prominent lateral foot displacement and partial paralysis of the hindlimb.

Locomotor defects in double-mutant animals were much more prominent than defects observed in any other genotype category with animals showing partial or full hindlimb paralysis. Double-mutant animals appeared to retain some flexibility of the hip joint, but did not demonstrate distal limb motility. Hindfeet in double-mutant animals were hyperextended either posteriorly or laterally; during locomotion, double-mutant animals used dorsal, ventral, and medial surfaces of the foot indiscriminately for load bearing. In addition, double-mutant animals were unable to hold or grasp objects such as wire cage bars or pencils with their hindfeet. Double-mutant animals were mildly responsive to toe pinch, but the rate of withdrawl was much slower and less complete than observed in wild-type or dual heterozygous animals.

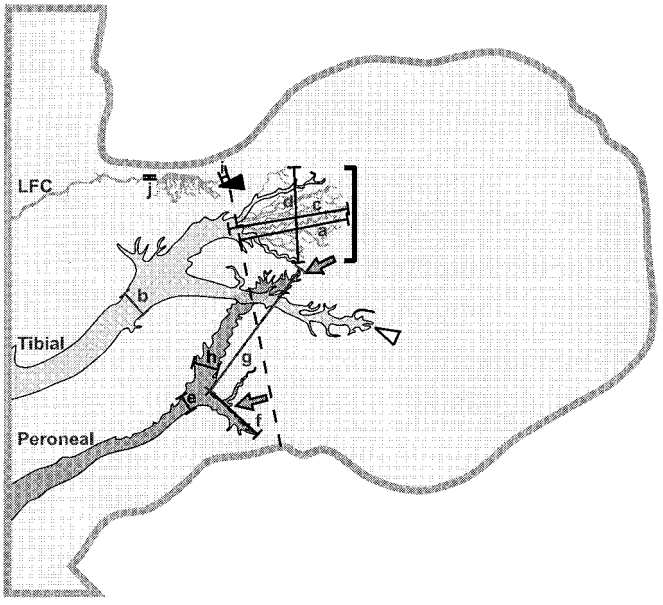

FIG. 2. Schematic representation of hindlimb innervation in the E12.5 mouse embryo illustrating the distal extent and branching patterns of the lateral femoral cutaneous (LFC, black arrowhead), tibial (large bracket and white arrowhead), and peroneal (dark arrows) nerves. Normally, the tibial and peroneal nerves overlap with each other in different planes within the hindlimb; in this figure, they are separated for clarity. The dashed line represents the boundary between limb and foot paddle. For analysis of peripheral nerve development, 10 measurements indicated by brackets were taken from these nerves as follows: a, tibial nerve length (measured relative to the foot paddle boundary); b, tibial nerve width; c, tibial arbor length; d, tibial arbor width; e, sciatic nerve width; f, superficial peroneal nerve length; g, deep peroneal nerve length; h, deep peroneal nerve width; i, LFC length (measured relative to the foot paddle boundary); j, LFC width.

Locomotor behavior was assessed using a modified open-field trial as described (de la Cruz *et al.*, 1999). Animals of all possible genotypes were scored for locomotion in an open field during three successive 5-min trials. Behaviors of wild-type, single, and dual heterozygous animals were indistinguishable from each other in these trials; all of these animals were observed to walk normally and to enter an average of 43 ± 17 quadrants during each locomotor trial. *Hoxa10*$^{-/-}$, *Hoxd10*$^{-/-}$, and *Hoxa10*$^{+/-}$/*Hoxd10*$^{-/-}$ mice entered 39 ± 12, 32 ± 17, or 33 ± 8 quadrants, respectively, fewer than control animals, but not statistically signficant. In contrast, *Hoxa10*$^{-/-}$/*Hoxd10*$^{+/-}$ and double-mutant animals entered significantly fewer quadrants (31 ± 4 or 18 ± 8 quadrants, respectively; $P < 0.05$, Student's t test), suggesting a decrease in locomotion in these animals.

Vertebral Transformations Following Hoxa10$^{+/-}$/*Hoxd10*$^{+/-}$ *Intercrosses*

Alizarin red-stained skeletons of 8-week-old mice of all genotypes were examined for both axial and appendicular alterations. Two major types of axial alterations affecting vertebral organization and pelvic position were observed. The typical posterior vertebral pattern of 13 thoracic, 6 lumbar, and 4 sacral (T13L6S4) vertebrae was observed in wild-type, single heterozygous, and dual heterozygous animals. *Hoxd10* mutant animals also demonstrate this pattern, but *Hoxa10* mutant animals typically had full or partial T14L5S4 patterns (Table 1). However, some *Hoxa10*$^{-/-}$ animals had 6 lumbar vertebrae, suggesting full penetration of the anterior transformation throughout the posterior axial skeleton (Table 1). Animals carrying three mutant alleles showed transformations of either thoracic or lumbar vertebrae, producing either a T14 or L7 phenotype both with and without alteration in the number of sacral vertebrae. All double mutants showed anterior vertebral transformation, most typically to produce 14 thoracic vertebrae, which in 30% of cases were accompanied by expansion in the number of lumbar vertebrae as well.

Changes in sacral identity have been previously reported for single-mutant animals (Rijli *et al.*, 1995; Satokata *et al.*, 1995; Favier *et al.*, 1996; Carpenter *et al.*, 1997). Sacral identity was also altered in dual heterozygous animals as well as in animals carrying three or four mutant alleles (Fig. 1). Dual heterozygous animals show occasional anterior transformation of S3 to S2 (S2* in Fig. 1E), similar to transformations observed in *Hoxa10* mutant animals (Fig. 1C). Animals carrying three mutant alleles show transformation of S2 to an S1 identity (S1* in Figs. 1F, H) as well as partial or full transformation of S1 to a lumbar identity (S1/L7* in Figs. 1F, H). *Hoxd10* mutants also show S2 to S1 transformations (Fig. 1G). S1 to L7 transformations alter the overall vertebral pattern by changing the number of lumbar vertebrae (Table 1). Double-mutant animals also show S1 to L7 transformations (Fig. 1I), which accompany more anterior lumbar to thoracic transformations producing animals with full or partial T14 vertebrae as well as anteriorly transformed lumbar and sacral vertebrae (Table 1).

Pelvic position was identified with respect to the vertebrae encased by the pelvis. Wild-type mice typically have a pelvis spanning L6-C1, but a few mice showed a slightly more posterior pelvic position, ending adjacent to C2. Single and dual heterozygous mice all showed similar pelvic positions. *Hoxd10*$^{-/-}$ animals had pelvises entirely in the more posterior wild-type position, while *Hoxa10*$^{-/-}$ animals demonstrated some variability in pelvic position with both more anterior and more posterior pelvic positions observed (Table 1). Animals carrying three mutant alleles also demonstrated a more variable pelvic position with *Hoxa10*$^{-/-}$/*Hoxd10*$^{+/-}$ mice showing slightly more anterior pelvic positions and *Hoxa10*$^{+/-}$/*Hoxd10*$^{-/-}$ mice showing slightly more posterior pelvic positioning. Twenty percent of double-mutant animals showed more posterior pelvic positions, with the pelvis shifted a full segment posteriorly in the most extreme cases.

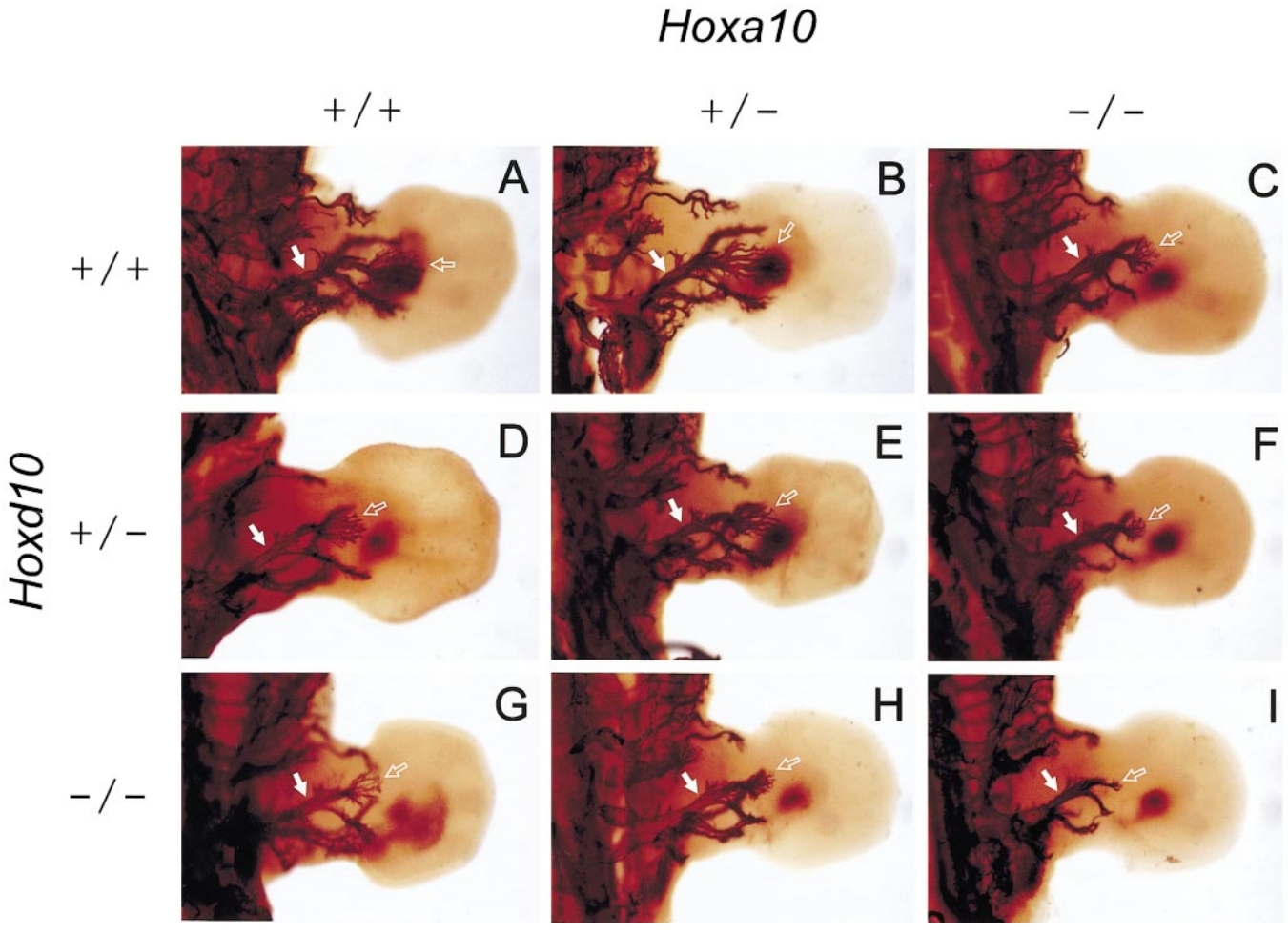

FIG. 3. Tibial nerve and arbor organization in E12.5 embryos produced from *Hoxa10*$^{+/-}$/*Hoxd10*$^{+/-}$ intercrosses; panels are arranged as in Fig. 1. Hindlimb peripheral nerves were labeled using antineurofilament antibodies. Tibial nerves prior to the bifurcation of the proximal tibial nerve are indicated by filled arrows and distal tibial arbors are indicated by open arrows in all panels. (A) Wild-type tibial nerve and distal tibial arbor. (B, D, E) Tibial nerves and tibial arbors in animals carrying a single-mutant allele at one or both loci resemble the wild-type pattern. (C, G) *Hoxa10*$^{-/-}$ and *Hoxd10*$^{-/-}$ animals have less mature tibial nerves and more disorganized tibial arbors. *Hoxd10*$^{-/-}$ animals (G) also appear to have fewer nerve fibers in the tibial arbor. (F, H) Animals carrying three mutant alleles have underdeveloped tibial arbors while double-mutant animals (I) demonstrate nearly complete absence of the tibial arbor.

Alterations in Hindlimb Innervation at E12.5

By Embryonic Day (E) 12.5, nerves derived from preaxial and postaxial nerve trunks in wild-type embryos have grown approximately two-thirds the length of the limb (Fig. 2). The distal portions of these nerves are readily visible in mouse hindlimbs labeled with anti-neurofilament antibodies (Figs. 3 and 4). In wild-type mice, the sciatic nerve, which is derived from the postaxial nerve trunk, has branched into the tibial and peroneal nerves. More distally, the peroneal nerve has divided into the superficial and deep peroneal branches and the tibial nerve has branched to provide motor innervation to the posterior thigh muscles. More distally, the tibial nerve has expanded into a terminal arbor in preparation for branching into the five plantar branches (Fig. 2, bracket; Fig. 3A, open arrow). Distal hindlimb peripheral nerve development appears significantly affected by alterations in both *Hoxa10* and *Hoxd10* activity. Single and dual heterozygous embryos have normal hindlimb nerve organization with well-defined preaxial and postaxial nerve trunks and well-developed terminal branches. However, animals mutant at either locus as well as animals carrying 3 or 4 mutant alleles show mild to signficant alterations in peripheral nerve organization (Figs. 3 and 4) with alterations in plantar branching and in the size and organization of the sciatic nerve trunk and peroneal branches.

Tibial nerve development. Tibial nerves in wild-type and single and dual heterozygous hindlimbs have typically

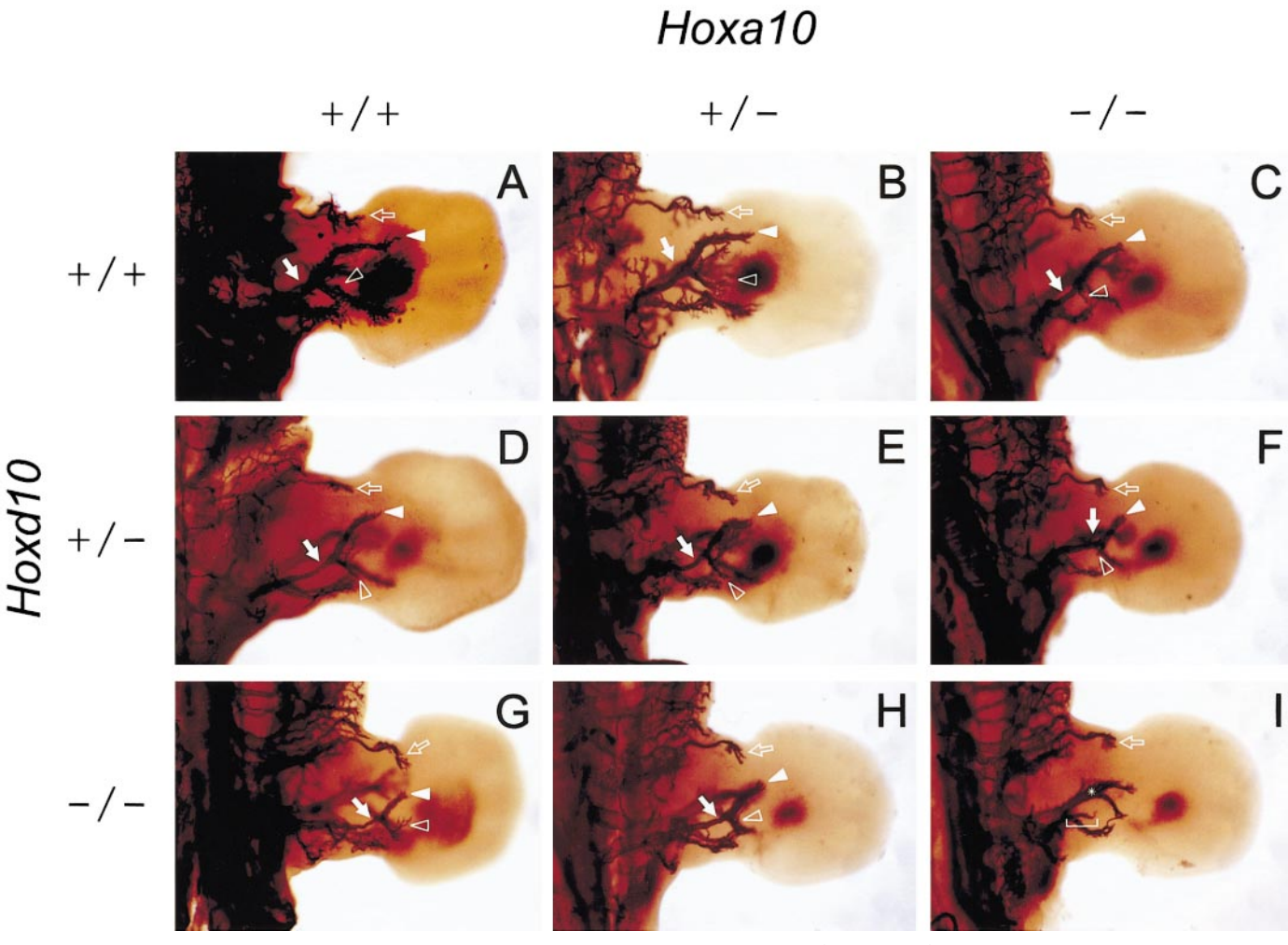

FIG. 4. Peroneal and LFC nerve organization in E12.5 embryos produced from *Hoxa10*$^{+/-}$/*Hoxd10*$^{+/-}$ intercrosses; panels are arranged as in Fig. 1. Panels in this figure are similar to those in Fig. 3, but were photographed at a different plane of focus to illustrate the position and branching patterns of the peroneal and LFC nerves. The proximal sciatic nerve (filled arrows) and its terminal branches the superficial (open arrowheads) and deep peroneal (filled arrowheads) nerves and the LFC nerve (open arrows) were examined in hindlimbs labeled with antineurofilament antibodies. (A) In wild-type animals, the superficial and deep peroneal nerves extend approximately one-third of the proximodistal extent of the foot paddle, while the LFC nerve has just reached the boundary between the distal limb and the foot paddle. *Hoxa10*$^{+/-}$ (B) and *Hoxd10*$^{+/-}$ (D) animals as well as dual heterozygous animals (E) show well-defined superficial and deep peroneal nerves as well as a robust LFC nerve. In *Hoxa10*$^{-/-}$ hindlimbs (C), the peroneal nerves are present, but not as well developed as in wild-type animals. *Hoxd10*$^{-/-}$ animals (G) display a thinning of the sciatic nerve and truncation of the distal peroneal nerves. *Hoxa10*$^{-/-}$/*Hoxd10*$^{+/-}$ (F) and *Hoxa10*$^{+/-}$/*Hoxd10*$^{-/-}$ (H) animals have shortened peroneal nerves and moderate alterations in the LFC nerve. Double-mutant animals (I) frequently show a much reduced distal sciatic nerve (bracket) and a complete absence of the superficial and deep peroneal branches. The asterisk indicates the position of the tibial nerve, which normally lies ventral to the sciatic nerve.

extended past the boundary between the limb and the foot paddle and have expanded into well-defined terminal arbors (Figs. 3A, B, D, E). The main tibial nerve trunks appear robust and the terminal arbors appear well differentiated, with numerous axon fascicles. In contrast, *Hoxa10* and *Hoxd10* mutant hindlimbs have less well-defined tibial arbors, with less distinct axon bundles (Figs. 3C, G), while *Hoxa10*$^{-/-}$/*Hoxd10*$^{+/-}$ and *Hoxa10*$^{+/-}$/*Hoxd10*$^{-/-}$ animals have shorter tibial nerves and greatly reduced tibial arbors (Figs. 3F, H). Six of the 11 *Hoxa10*$^{-/-}$/*Hoxd10*$^{-/-}$ hindlimbs examined completely lack distal tibial arbors (Fig. 3I); in the remaining hindlimbs, the arbors were clearly smaller and less well organized than in control hindlimbs.

The extent of tibial nerve growth was examined by measuring the length of the tibial nerve with respect to the position of the boundary between the limb and the foot paddle (Fig. 2). Tibial nerve width was measured prior to the emergence of the proximal tibial branch (Fig. 2). The tibial nerve extended an average of 229.4 μm past the foot paddle boundary in wild-type animals (Fig. 5A). Tibial nerve length

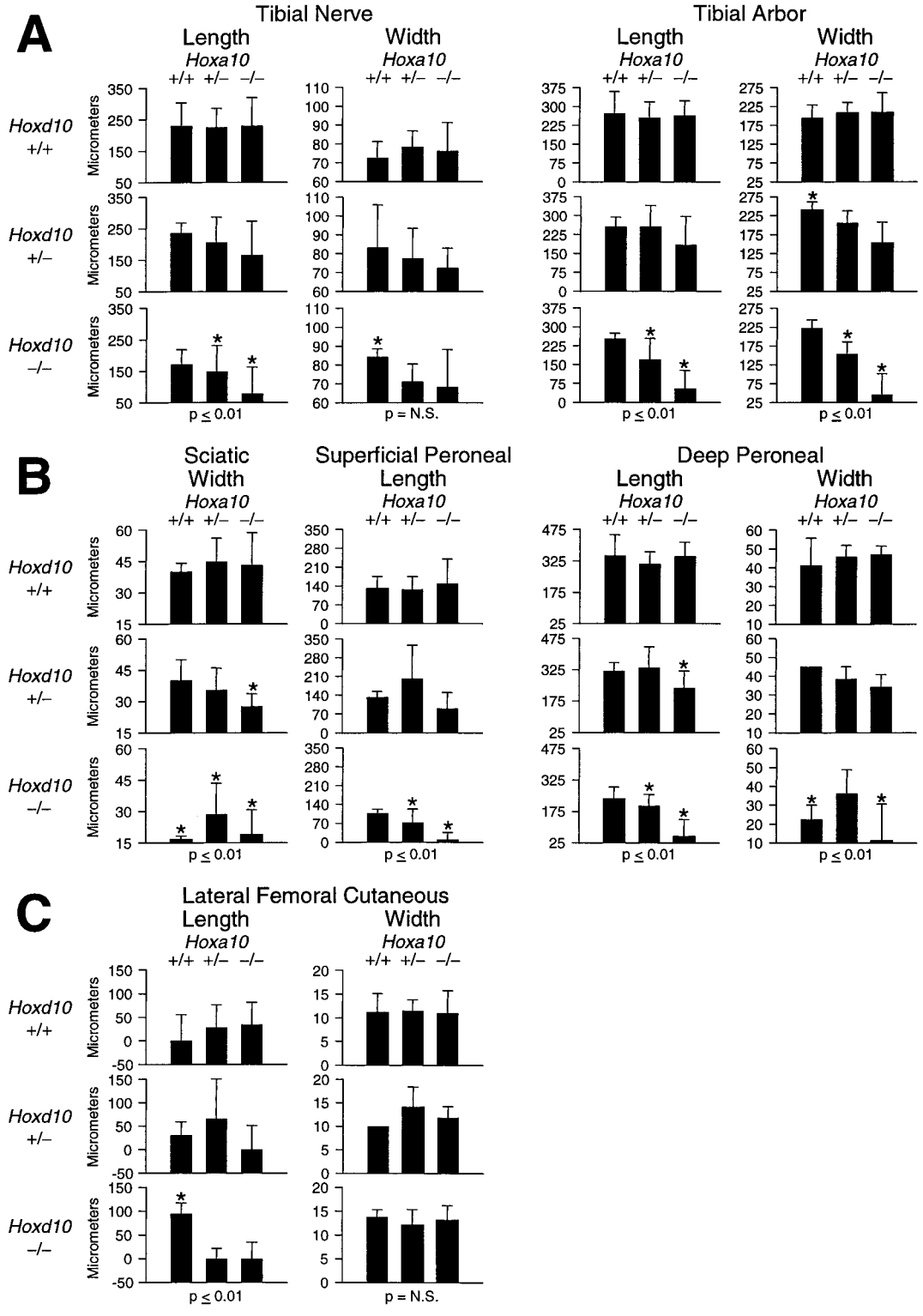

FIG. 5. Graphic representation of nerve parameter measurements in animals derived from *Hoxa10*$^{+/-}$/*Hoxd10*$^{+/-}$ intercrosses. Nerve dimensions were measured in micrometers as indicated in Fig. 2. Mean and standard error for each variable were plotted in groups to show alterations in a single variable across the spectrum of genotypes derived from *Hoxa10*$^{+/-}$/*Hoxd10*$^{+/-}$ intercrosses. *Hoxa10* genotypes are distributed left to right and *Hoxd10* genotypes are distributed top to bottom. The average values for each genotype were compared to wild-type values using two-sample Student's *t* test assuming unequal variance; values that are significantly different from wild-type values ($P < 0.05$) are indicated with an asterisk. The overall distribution of values measured for a single variable was analyzed for significance using ANOVA; ANOVA values are presented below the graph for each variable. (A) Tibial nerve measurements. (B) Sciatic and peroneal nerve measurements. (C) Lateral femoral cutaneous nerve measurements.

was decreased somewhat in *Hoxa10*$^{-/-}$/*Hoxd10*$^{+/-}$ hindlimbs, and was significantly decreased in *Hoxa10*$^{+/-}$/*Hoxd10*$^{-/-}$ and *Hoxa10*$^{-/-}$/*Hoxd10*$^{-/-}$ hindlimbs (Fig. 5A). In comparison, tibial nerve width was similar in embryos of most genotypes (Fig. 5A); however, *Hoxd10* mutant animals had the widest tibial nerves, averaging 84.3 μm wide. While this measurement was significantly different from wild-type values ($P < 0.05$, Student's t test), the overall distribution of tibial nerve width measurements for all genotypes was not statistically significant (Fig. 5A).

At its distal end, the tibial nerve expands into a terminal arbor which subsequently divides into five branches to innervate the plantar muscles of the toes. The dimensions of this arbor were measured to examine distal tibial development in contrast to overall tibial nerve growth as examined above. The position of the arbor was somewhat variable, sometimes beginning to expand proximal to the foot paddle boundary and sometimes more distally. Arbor length averaged 273.6 μm in length and 195 μm in width in wild-type hindlimbs, with similar dimensions observed in hindlimbs of most genotypes (Fig. 5A). *Hoxa10*$^{+/-}$/*Hoxd10*$^{-/-}$ hindlimbs showed significant reductions in arbor length and width, while double-mutant animals often showed complete failure of arbor expansion, with 6 of 11 limbs examined lacking a terminal tibial nerve arbor.

Distal sciatic nerve development. Distal sciatic nerve development at E12.5 was robust in wild-type animals, with clearly delineated branches which extend into the foot paddle past the tibia/fibula limb segment (Fig. 4A). The sciatic nerve appeared substantially thinner in *Hoxd10*$^{-/-}$ animals (Fig. 4G) as well as in animals carrying three mutant alleles (Figs. 4F, H). Double-mutant animals consistently showed alterations in superficial and deep peroneal nerve patterning with 8 of 11 double-mutant hindlimbs lacking these nerves (Fig. 4I).

Distal sciatic nerve width, deep peroneal nerve width and length, and superficial peroneal length (Fig. 2) were all measured to quantify sciatic nerve and terminal branch development. Sciatic nerve width averaged 40 μm in wild-type animals at E12.5 (Fig. 5B). *Hoxd10* mutants, as well as animals carrying 3 or 4 mutant alleles, showed significant reductions in the width of the sciatic nerve, as compared to wild-type values, with *Hoxd10*$^{-/-}$ and *Hoxa10*$^{-/-}$/*Hoxd10*$^{-/-}$ hindlimbs having sciatic nerve widths that were less than half the diameter of wild-type nerves (Fig. 5B). The deep peroneal nerve extended an average of 351.4 μm past its branch point in wild-type embryos and averaged 41.4 μm in width. Deep peroneal nerve lengths in *Hoxa10*$^{+/-}$/*Hoxd10*$^{-/-}$ and *Hoxa10*$^{-/-}$/*Hoxd10*$^{+/-}$ animals were reduced to an average of 202.5 and 236.7 μm, respectively; both values are signficantly different from wild-type measurements ($P < 0.05$, Student's t test). Deep peroneal nerve widths were similar for most genotypes; however *Hoxd10* mutant hindlimbs had significantly narrower deep peroneal nerves (Figs. 4G and 5B). The deep peroneal nerve was missing in 8 of the 11 limbs examined in *Hoxa10*$^{-/-}$/*Hoxd10*$^{-/-}$ animals (Fig. 4I); in the 3 hindlimbs where a deep peroneal nerve could be identified, the length of this nerve varied from 130 to 200 μm. The widths of these three nerves varied from 10 to 45 μm, suggesting that a few nerves could attain near wild-type dimensions.

The superficial peroneal was also signficantly reduced in length in *Hoxa10*$^{+/-}$/*Hoxd10*$^{-/-}$ hindlimbs as compared to wild-type limbs, averaging 74 μm in *Hoxa10*$^{+/-}$/*Hoxd10*$^{-/-}$ hindlimbs and 129.2 μm in wild-type hindlimbs. The superficial peroneal nerve was absent in 8 out of 11 double-mutant hindlimbs (Fig. 4I). Due to limb positioning, the length of this nerve could only be accurately measured in one limb; in this limb, the superficial peroneal branch was 70 μm long.

Lateral femoral cutaneous nerve development. The lateral femoral cutaneous (LFC) nerve branches from the dorsal nerve trunk within the thigh to provide sensory innervation for the proximal thigh (Fig. 4, open arrows). The length of the LFC nerve was measured with respect to the boundary between the limb and the foot paddle, similar to tibial nerve measurements. In wild-type animals, the LFC nerve grew to approximately the position of this boundary on average (LFC length = 1.9 μm; Fig. 5C). *Hoxd10* mutant animals had lateral femoral cutaneous nerves which grew more distally into the hindlimb autopod, but animals of all other genotypes demonstrated LFC nerve growth which was not significantly different from that observed in wild-type animals. The width of this nerve was also not signficantly different in animals of all genotypes, suggesting that some hindlimb nerves may be relatively unaffected by mutations in *Hoxa10* and *Hoxd10*.

Hindlimb Innervation at E13.5

By E13.5, the tibial nerve normally subdivides proximally into two major nerve trunks and distally into 5 branches to innervate the plantar muscles of the toes in wild-type embryos (Fig. 6A). Tibial nerve development is disrupted in *Hoxa10*$^{-/-}$/*Hoxd10*$^{-/-}$ animals such that the tibial nerve remains bundled into a single nerve trunk and terminal branching is disrupted (Figs. 6C, D). Widespread axonal branching is evident in the distal tibial arbor and axons appear spread over the extent of the arbor rather than aggregated into tight fascicles. In addition, the terminal arbor appears more sparsely populated with axons than in wild-type arbors, suggesting that some component of tibial axons is missing.

Sciatic nerve patterning is also disrupted at E13.5 in double-mutant animals. Normally, the superficial peroneal branch has arborized extensively and the deep peroneal branches of the sciatic nerve have grown distally into the developing foot (Fig. 7A). In the double-mutant animals examined, both branches of the sciatic nerve were significantly underdeveloped or entirely absent (Figs. 7C, D). These observations suggest that the defects observed in the sciatic nerve and its terminal branches are permanent and do not simply reflect a developmental delay in double-mutant animals.

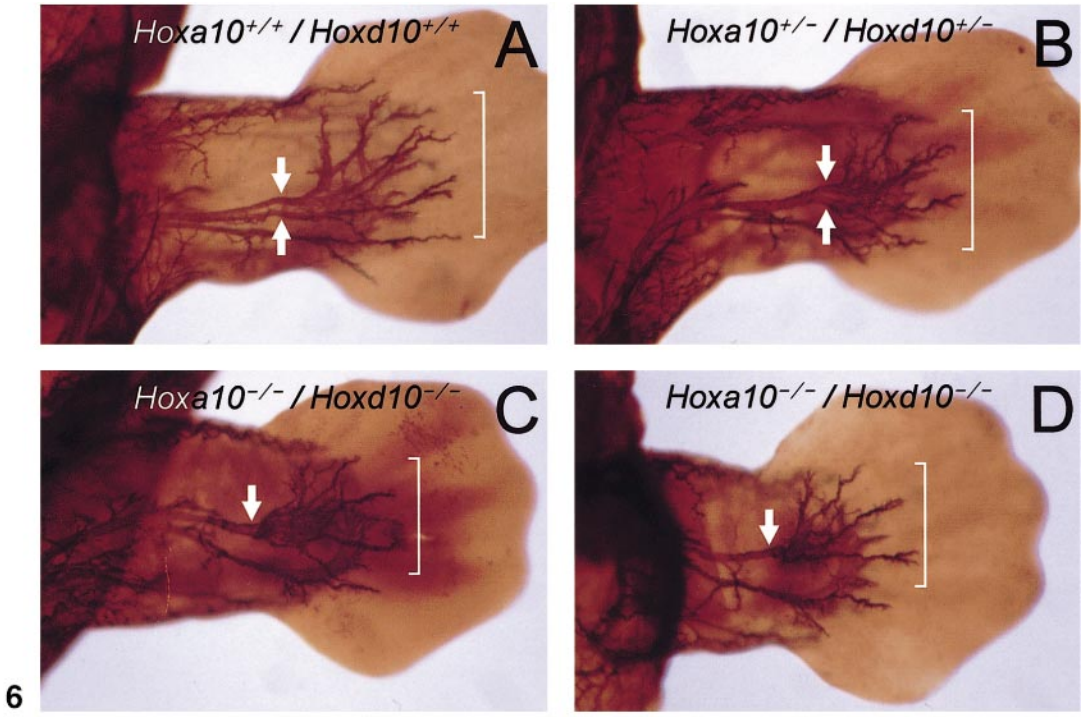

6

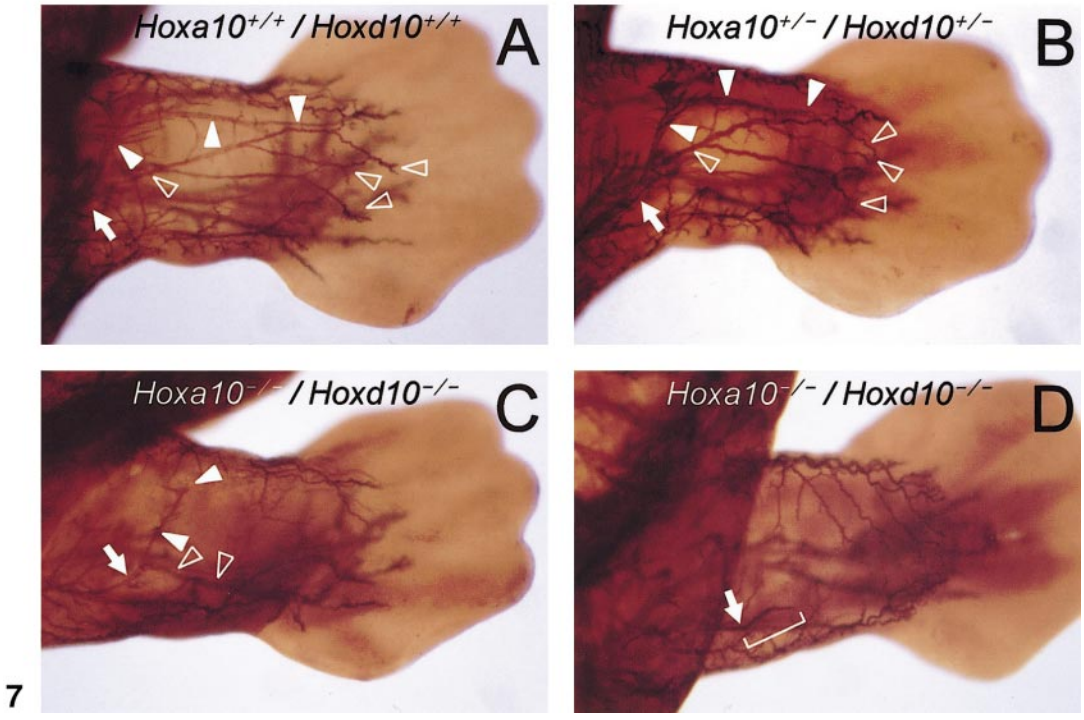

7

FIG. 6. Tibial nerve and arbor organization in *Hoxa10*$^{-/-}$/*Hoxd10*$^{-/-}$ hindlimbs at E13.5. labeled with anti-neurofilament antibodies. (A) Tibial nerves in wild-type animals divide into two trunks (paired arrows) prior to expansion into the distal tibial arbor. At this age, fibers in the tibial arbor (bracket) have fasciculated into 5 branches destined to innervate the plantar muscles of the feet. *Hoxa10*$^{+/-}$/*Hoxd10*$^{+/-}$ animals (B) have tibial nerves and arbors resembling those seen in wild-type animals. Double-mutant animals (C, D) have a single tibial nerve trunk (arrow). Fibers in the distal tibial arbor appear defasciculated (C) and the terminal branches appear thinner and shorter (D) than in wild-type animals.

FIG. 7. Sciatic and peroneal nerve organization in *Hoxa10*$^{-/-}$/*Hoxd10*$^{-/-}$ hindlimbs at E13.5. In wild-type hindlimbs (A) the main trunk of the sciatic nerve (arrow) branches into the superficial (open arrowheads) and deep (filled arrowheads) peroneal nerves. Both peroneal nerves undergo profuse branching to provide sensory and motor innervation for the distal part of the hindlimb. *Hoxa10*$^{+/-}$/*Hoxd10*$^{+/-}$ hindlimbs (B) show superficial and deep peroneal nerve projections similar to those seen in wild-type hindlimbs. *Hoxa10*$^{-/-}$/*Hoxd10*$^{-/-}$ hindlimbs (C, D) contain much thinner sciatic nerve trunks (arrows) and greatly reduced peroneal branches (arrowheads). In some cases, the sciatic nerve appears not to divide distally and only a small terminal sciatic projection is evident (bracket in D).

TABLE 2

Hindlimb Skeletal Phenotypes Following *Hoxa10*$^{+/-}$/*Hoxd10*$^{+/-}$ Intercrosses

Hoxa10	+/+	+/−	+/+	+/−	−/−	+/+	−/−	+/−	−/−
Hoxd10	+/+	+/+	+/−	+/−	+/+	−/−	+/−	−/−	−/−
Limbs examined	18	16	2	20	36	8	36	30	32
Femur									
Greater trochanter misshapen				20	72.2	25	27.8	46.7	75
Trochanter tertius +				40	27.8	25	11.1	46.7	12.5
extended distally ++					38.9		22.2	13.3	18.8
+++					11.1		38.9		68.8
Knee joint									
Patella shifted proximally				10	5.6	75	22.2	53.3	37.5
Anterior sesamoid							5.6	6.7	
Patella shifted laterally									6.3
Lateral sesamoid: missing							5.6		
ectopic					11.1		5.6		6.3
Medial sesamoid: missing					55.6		33.3		62.5
reduced			12.5		5.6				6.3
ectopic					5.6		5.6		6.3
Tibia									
Medial malleolus misshapen					5.6				
Bowed or twisted								6.7	6.3
Tibia/Fibula									
Bone fusion: slightly diminished				10	33.3		11.1	13.3	12.5
diminshed fusion					33.3		16.7	6.7	25
full separation									12.5
Extra distal sesamoid					22.2	25	16.7		6.3
Fibula									
Thicker/straighter					22.2		16.7	13.3	37.5
Bowed					5.6				18.8
Proximal cartilage enlarged					27.8				
Lateral malleolus misshapen		12.5			27.8		22.2		12.5
Distal hindlimb rotations									
Tibia/fibula −[a]						25	22.2	26.7	25
Fibula −							22.2		6.3
Tibia/fibula +[b]				35	11.1	25	11.1	40	6.3
Distal T/F +							5.6	13.3	25
Hindfoot inward	11.1			10	11.1	25	38.9	50	37.5
Hindfoot outward				5		25	11.5	3.3	

Note. Percentage of animals derived from *Hoxa10*$^{+/-}$/*Hoxd10*$^{+/-}$ intercrosses demonstrating alterations in hindlimb skeletal elements.

[a] Less than normal rotation.

[b] Greater than normal rotation.

Hindlimb Skeletal Alterations

Appendicular skeletons were examined in 8-week-old mice stained with alizarin red. Alterations were noted in both forelimb and hindlimb skeletons. Hindlimb alterations will be described here in conjunction with observations made on hindlimb innervation; forelimb alterations will be described elsewhere. In the hindlimb, alterations were observed in the stylopod and the zeugopod, affecting the femur, the knee joint, and the tibia/fibula. Alterations in the greater trochanter were observed in 72.2% of *Hoxa10*$^{-/-}$ animals and 75% of *Hoxa10*$^{-/-}$/*Hoxd10*$^{-/-}$ mice; *Hoxd10*$^{-/-}$ and animals carrying 3 out of 4 mutant alleles also showed alterations in the greater trochanter, but at lower penetrance. Alterations in the trochanter tertius were also observed with some frequency, with the most severe alterations seen in *Hoxa10*$^{-/-}$, *Hoxa10*$^{-/-}$/*Hoxd10*$^{+/-}$, and double-mutant animals. In most double-mutant animals, the trochanter tertius was greatly expanded, extending continuously to the knee. Animals carrying 3 or 4 mutant alleles demonstrated proximal shifts of the patella, similar to those seen in *Hoxd10* mutants (Carpenter *et al.*, 1997) as well as occasional lateral shifts (Table 2). The lateral sesamoid was missing in one *Hoxa10*$^{-/-}$/*Hoxd10*$^{+/-}$ animal, while extra lateral sesamoid bones were present in *Hoxa10*$^{-/-}$, *Hoxa10*$^{-/-}$/*Hoxd10*$^{+/-}$, and double-mutant animals. The medial sesamoid bone was often reduced or

missing in *Hoxa10*$^{-/-}$, *Hoxa10*$^{-/-}$/*Hoxd10*$^{+/-}$, and double-mutant animals as well, although a few animals of these genotypes had extra medial sesamoid bones.

More distal alterations affected both the tibia and the fibia, producing alterations in bone morphology and distal limb placement. Normally, the tibia and fibula are fused at their distal ends, but the extent of bone fusion was diminished in *Hoxa10*$^{-/-}$ animals, as well as in animals carrying 3 or 4 mutant alleles. Full separation between the tibia and fibula was observed at low penetrance in double-mutant animals as well. Tibial malformations were limited to alterations in the medial malleolus and bowing or twisting of the tibia in a few animals. The fibula appeared thicker and straighter or bowed in double-mutant animals, and at lower penetrance in *Hoxa10*$^{-/-}$ animals and in animals carrying 3 mutant alleles. Proximal alterations in the medial malleolus and cartilage were also observed, but appeared at slightly higher frequency in *Hoxa10*$^{-/-}$ animals than in animals of any other genotype.

During embryonic development, both proximal and distal elements of the hindlimb rotate from their original position to produce limbs appropriately positioned for tetrapedal gait (Lance-Jones, 1979; Kaufman and Bard, 1999). Between E12.5 and E17.5, the proximal part of the hindlimb rotates medially approximately 90°, while the distal part of the hindlimb independently rotates 180° (Kaufman and Bard, 1999), to produce a weight-bearing, medially positioned limb and foot. Animals derived from *Hoxa10*$^{+/-}$/*Hoxd10*$^{+/-}$ intercrosses show significant abnormalities in distal hindlimb position, suggesting alterations in the distal rotation of the hindlimb. Rotations were scored qualitatively as overrotations or underrotations and are indicated with + or − designations in Table 2. The tibia and fibula as a unit appear over- or underrotated in *Hoxd10*$^{-/-}$ animals, as well as in animals carrying 3 mutant alleles and in double-mutant animals. This rotation can affect the entire tibia and fibula, or only the distal part. In some animals, the fibula appears to rotate medially independently of the tibia. Foot position is also affected in these animals, suggesting abnormal rotation of the foot as well. A large number of animals show inward rotation of the foot, such that the lateral surface of the foot rotates medially. Similar placement is occasionally observed in wild-type animals (Table 2), but the penetrance and degree of rotation are greatly increased in animals carrying 2, 3, or 4 mutant alleles. Similar foot position could also be generated by underrotation of the zeugopod as seen in *Hoxd10*$^{-/-}$ animals and in animals carrying 3 or 4 mutant alleles. Outward foot rotations were also observed, but at lower penetrance.

DISCUSSION

Four pairs of paralogous *Hoxa* and *Hoxd* genes exist in mice. Previous studies have shown that genes in 3 of these paralogous pairs interact to regulate limb and axial development. In this study, we have examined the interactions between the genes of the remaining paralogous pair, *Hoxa10* and *Hoxd10*. Our results show that animals derived from intercrosses of *Hoxa10*$^{+/-}$/*Hoxd10*$^{+/-}$ parents which carry 2, 3, or 4 mutant alleles show a spectrum of hindlimb alterations including changes in locomotor behavior, skeletal organization, and peripheral innervation. As is seen with other pairs of paralogous genes, our observations support the hypothesis that combinatorial interactions between members of the *Hoxa* and *Hoxd* gene cluster regulate regional patterning in the developing limb. Our results show that the effects of these genes are not limited to a single tissue type within the limbs, but suggest regulation of several different components of the developing limb. These interactions may reflect combinatorial regulation of downstream molecules such as N-CAM or other growth-regulating or cell adhesion molecules.

Locomotor Alterations Produced by Hoxd10 Are Exacerbated by Mutation in Hoxa10

Alterations in locomotor behavior have been described for mice carrying a mutation in *Hoxd10* (Carpenter *et al.*, 1997); locomotion in *Hoxa10* mutant mice appears normal (Rijli *et al.*, 1995; Satokata *et al.*, 1995; this study). Gait defects appear more pronounced in animals carrying an increasing complement of *Hoxa10* and *Hoxd10* mutant alleles, with animals carrying 3 out of 4 mutant alleles demonstrating mildly impaired mobility and altered locomotion and double-mutant animals demonstrating significant decreases in mobility and highly abnormal locomotion. Severe gait defects were observed in only 17% of *Hoxd10* mutant animals (Carpenter *et al.*, 1997), while all *Hoxa10/Hoxd10* double-mutant animals have severe gait defects, which were in all cases more severe than those observed in *Hoxd10* single-mutant animals. These increases in the severity of locomotor defects suggest that *Hoxa10* and *Hoxd10* interact to affect locomotion in animals carrying mutations in both genes.

Locomotor defects may stem from alterations in bone or muscle development and placement or from changes in central or peripheral nervous system organization and projection. Our current observations document skeletal and peripheral nervous system changes; both defects are likely to affect locomotion. The abnormal hindfoot rotations observed during locomotion in animals carrying three or four mutant alleles are likely to stem from the abnormal rotations of the tibia and fibula observed in skeleton preparations. Hyperextension of the hindfoot may stem from alterations in bone rotation or from loss of the distal branches of the sciatic nerve trunk. The deep peroneal nerve, which is frequently absent in double-mutant animals, normally innervates the anterolateral extensor muscles which regulate dorsiflexion of the foot. Loss of this nerve would create hyperextension of the hindfoot as is observed in double-mutant animals. Changes were also observed in the distal tibial nerve, which innervates the plantar muscles of the foot; changes in this innervation may contribute to the abnormal foot postures observed during locomotion. One additional possibility is that changes in

hindlimb musculature could alter locomotor behavior. Preliminary observations suggest no major defects in hindlimb muscle position (A. Lin and E. M. Carpenter, unpublished observations), though muscle mass in double-mutant hindlimbs appears reduced. Changes in peripheral innervation might also contribute to the loss of muscle mass due to a decrease in muscle activation.

Hoxa10 and Hoxd10 Independently Regulate Axial Patterning in Lumbar and Sacral Domains

Hoxa10 and *Hoxd10* are normally expressed in overlapping domains encompassing lumbar and sacral paraxial mesoderm, with rostral limits of expression at the level of the L1 spinal segment (Dollé and Duboule, 1989; Bensen *et al.,* 1995). Mutations in *Hoxa10* produce anterior vertebral transformation affecting vertebrae from position 21 (the wild-type L1 position) through position 26 (Rijli *et al.,* 1995; Satokata *et al.,* 1995; Favier *et al.,* 1996) with a return to normal register at position 27 and more posteriorly. A mutation in *Hoxd10* primarily affects sacral vertebrae, producing anterior transformation of vertebrae at position 28 and more posteriorly (Carpenter *et al.,* 1997). Based on these observations, *Hoxa10* and *Hoxd10* appear to regulate vertebral identity in different axial domains despite their largely overlapping expression patterns. Animals carrying mutations in both *Hoxa10* and *Hoxd10* showed vertebral transformation in both lumbar and sacral domains. Anterior transformation of the vertebra at position 21 from lumbar to thoracic morphology was observed in all double mutants, with additional transformations of more posterior vertebrae extending through sacral levels in 88% of double-mutant animals. Animals carrying 3 out of 4 mutant alleles showed similar transformations, though at lower penetrance, with $Hoxa10^{-/-}/Hoxd10^{+/-}$ animals showing more rostral transformations and $Hoxa10^{+/-}/Hoxd10^{-/-}$ animals showing more caudal transformations. These observations suggest relatively independent effects of *Hoxa10* and *Hoxd10* in regulating vertebral identity. Combining mutations did not produce more widespread or severe vertebral transformations, but did increase the penetrance slightly over transformations observed in single-mutant animals.

One additional variable potentially involved in lumbar and sacral axial patterning might be the expression and activity of *Hoxc10,* the third member of the *Hox10* paralogous gene family. *Hoxc10* is expressed axially at lumbar and sacral levels (Goto *et al.,* 1993; Peterson *et al.,* 1994); however, inactivation of *Hoxc10* produces only mild vertebral transformations (Suemori and Noguchi, 2000; S. L. Hostikka, unpublished observations). Deletion of the entire *HoxC* gene cluster only weakly affects axial patterning (Suemori and Noguchi, 2000), suggesting a relatively minor role for these genes in determining vertebral identity.

Another axial alteration observed in *Hoxa10/Hoxd10* double-mutant animals was a posterior shift in pelvic position. The pelvis normally develops adjacent to the vertebrae at positions 27–33 (the wild-type L6-C1 vertebrae), developing an articulation with sacral vertebrae between E12.5 and E13.5 (Lance-Jones, 1979). Pelvic position may be dictated by axial cues, therefore the shift in pelvic position may reflect the identity transformation undergone by the adjacent vertebrae. With anterior transformation of vertebral identity, a posterior shift of the pelvis would not be unexpected.

Hoxa10 and Hoxd10 Act Independently and in Combination to Regulate Hindlimb Skeletal Development

Hoxa10 and *Hoxd10* independently affect hindlimb skeletal development, with defects confined primarily to the stylopod and zeugopod (Favier *et al.,* 1996; Carpenter *et al.,* 1997; this study). However expression of these genes appears largely confined to the mesenchyme and perichondral condensations of the zeugopod (Dollé and Duboule, 1989; Yokouchi *et al.,* 1991; Bensen *et al.,* 1995). Both $Hoxa10^{-/-}$ and $Hoxd10^{-/-}$ mice show alterations in the greater trochanter and the trochanter tertius of the femur, with changes in these structures appearing with greater penetrance in $Hoxa10^{-/-}$ mice. Animals carrying 3 out of 4 mutant alleles and double-mutant animals show similar changes, with somewhat increasing severity in alterations of the trochanter tertius. In the knee joint, *Hoxa10* animals showed alterations in the sesamoid bones, while *Hoxd10* mutant animals showed alterations in the position of the patella (Favier *et al.,* 1996; Carpenter *et al.,* 1997). Animals carrying 3 out of 4 mutant alleles showed similar alterations, with alterations in the sesamoid bones predominating in $Hoxa10^{-/-}/Hoxd10^{+/-}$ animals and alterations in patellar position predominating in $Hoxa10^{+/-}/Hoxd10^{-/-}$ animals. Double-mutant animals showed both phenotypes, though the patellar shifts where observed about half as frequently as in $Hoxd10^{-/-}$ animals. These observations suggest that *Hoxa10* and *Hoxd10* play independent, noncooperative roles in patterning the proximal hindlimb and knee joint, as, with the exception of the trochanter tertius remodeling, no significant increases in severity or penetrance were observed following combination of mutations in both *Hoxa10* and *Hoxd10.* These observations also suggest that alterations in limb patterning may occur outside of the domains where *Hoxa10* and *Hoxd10* are expressed. While these alterations may signify that not all areas of *Hoxa10* and *Hoxd10* expression in the developing hindlimb have been identified, they may also suggest that patterning and cell fate decisions in the proximal hindlimb may arise as secondary consequences of inactivation of more distally expressed genes.

Alterations in the morphology of the tibia and fibula appear predominantly dictated by *Hoxa10* function, as these morphological changes are present in $Hoxa10^{-/-}$, $Hoxa10^{-/-}/Hoxd10^{+/-}$, and double-mutant animals, while these alterations are rare in $Hoxd10^{-/-}$ animals. The severity of the alterations appears not to increase significantly between *Hoxa10* single-mutant animals and *Hoxa10/Hoxd10* double-mutant animals, suggesting that all of these morphological changes are derived from loss of *Hoxa10*

activity. In contrast, *Hoxd10* appears to predominate in determining the position of the lower part of the hindlimb in that distal hindlimb rotations are observed in $Hoxd10^{-/-}$ animals and in double-mutant animals with no apparent change in penetrance and appear to be relatively unaffected by inclusion of mutations in *Hoxa10*. These observations suggest that *Hoxa10* and *Hoxd10* play separate roles in determining the shape and position of the tibia and fibula, with *Hoxa10* acting on bone morphology and *Hoxd10* acting to determine bone position.

The bone remodeling present in *Hoxa10/Hoxd10* double-mutant animals is likely to arise during condensation, one of the primary phases of skeletogenesis. During condensation, dispersed mesenchymal cells aggregate to form recognizable precursors of skeletal elements. *Hox* genes may be involved in condensation directly through regulation of chondrocyte proliferation or indirectly through regulation of adhesion molecules such as N-CAM or N-cadherin involved in cellular aggregation (reviewed in Hall and Miyake, 2000). *Hoxa10* and *Hoxd10* appear to regulate condensation in different skeletal domains, with *Hoxa10* active in modeling the femur and proximal tibia and fibula and *Hoxd10* active in modeling the patella and distal tibia and fibula. Overlapping expression and regulation, such as may occur in the trochanter tertius and the tibia and fibula, suggest that these two genes may interact to pattern these regions of the limb.

Hindlimb Peripheral Innervation Is Regulated by Both Hoxa10 and Hoxd10

Hindlimb innervation is extensively affected in $Hoxa10^{-/-}$/$Hoxd10^{-/-}$ animals, with defects observed in the distal elements of the tibial and sciatic nerves. Nervous system alterations have been previously described for both $Hoxa10^{-/-}$ and $Hoxd10^{-/-}$ animals, with $Hoxa10^{-/-}$ animals demonstrating a transformation of a spinal segmental nerve (Rijli *et al.*, 1995) and $Hoxd10^{-/-}$ animals demonstrating alterations in spinal segmental identity and in peripheral nerve projections (Carpenter *et al.*, 1997). In most $Hoxa10^{-/-}/Hoxd10^{-/-}$ hindlimbs, the tibial nerve was shortened and showed a truncated distal arbor, while the peroneal nerves were reduced or deleted. $Hoxd10^{-/-}$ animals also demonstrated alterations in these two nerves, but not to the extent observed in double-mutant animals. These observations suggest alterations both in axonal growth and in nerve branching, with combinatorial interactions between *Hoxa10* and *Hoxd10* producing alterations in both of these aspects of peripheral nerve development. However, our results also suggest independent effects of the two genes on the different elements of the peripheral nervous system.

Tibial nerve patterning appears to be dually regulated by both *Hoxa10* and *Hoxd10* in that the length of the tibial nerve and the length and width of its terminal arbor appear more dramatically affected in double-mutant animals as compared to wild-type or to either single mutant. Measurements of tibial nerve width, however, suggest an independent effect of *Hoxd10* which is not observed in the double mutants. The tibial nerve is wider in $Hoxd10^{-/-}$ animals than in either wild-type or double-mutant animals, suggesting that *Hoxd10* alone affects tibial nerve width, with that effect negated by the addition of a mutation in *Hoxa10*. One possible mechanism to explain these observations is the differential regulation of cell adhesion molecules in the developing peripheral nervous system. *Hox* genes have been shown to regulate the expression of cell adhesion molecules such as N-CAM, Ng-CAM, and L1 (reviewed in Edelman and Jones, 1998). One of these adhesion molecules, N-CAM, participates in regulating axonal adhesion within fascicles; in particular, the degree of adhesivity can be regulated by modulating the polysialic acid content of N-CAM (Tang *et al.*, 1994). In the absence of *Hoxd10*, axon-axon adhesion may be affected to decrease fasciculation, producing a wider nerve trunk as is visible in $Hoxd10^{-/-}$ animals. Mitigation of this effect by the inclusion of mutant *Hoxa10* could reflect a positive/regulation of N-CAM, similar to that demonstrated by *Hoxb8* and *Hoxb9* (Edelman and Jones, 1995).

Both superficial and deep peroneal nerves are affected in double mutants, with both nerves deleted or decreased more significantly in double-mutant animals than in wild-type or single mutant animals. However, *Hoxd10* alone appears to regulate the width of the sciatic nerve prior to its distal branch point. The width of the sciatic nerve is decreased in *Hoxd10* mutants to approximately the same extent as it is in double-mutant animals, suggesting that addition of a mutation in *Hoxa10* has no additional effect on sciatic nerve width. Deep peroneal width is also decreased in *Hoxd10* mutants (though not significantly), but the deep peroneal nerve is thinner in double mutants than in *Hoxd10* mutants alone.

The observed decreases in nerve width and deletion of terminal branches suggest either a loss of axons within the developing peripheral nerves or a change in the distribution of these fibers. Axonal loss could reflect a lack of cell proliferation or specification in the developing spinal cord to produce appropriate numbers of motor neurons. Histological examination of newborn animals suggests that loss of *Hoxd10* activity selectively depletes lumbar lateral motor column motor neuron populations (E. M. Carpenter, unpublished observations), suggesting possible effects on cell proliferation or cell survival. Loss of distal sciatic nerve branches might also reflect changes in the regulation of processes related to neurite outgrowth such as fasciculation or a delay in outgrowth. L1 and N-CAM have specific effects on neurite extension and growth cone protrusion (Takei *et al.*, 1999); the observed lack of neurite outgrowth into the sciatic nerve could reflect loss of L1 or N-CAM activation by *Hoxa10* and *Hoxd10*. Alternatively, axonal growth and extension could procede normally, with subsequent losses in neurites stemming from a lack of peripheral targets, as might be generated by remodeling the mesenchymal elements of the hindlimb. However, the reductions in tibial and sciatic branches occur prior to the period of lumbar motor column cell death (Lance-Jones, 1982), sug-

gesting that fiber losses do not occur as a result of target loss. A delay in nerve outgrowth also appears unlikely given that changes in distal tibial and peroneal nerve development are maintained between E12.5 and E13.5, while normal growth is observed for more proximal sciatic nerve branches. Observations in *Hoxd10*$^{-/-}$ animals also suggest that changes in the deep peroneal nerve are maintained into adulthood (Carpenter *et al.*, 1997). One additional possibility is that changes in nerve length might reflect changes in limb segment length. This is unlikely, because the femur and tibia/fibula do not appear shorter in mutant animals, as might be expected if limb segments were shortened.

In contrast to tibial and sciatic nerve alterations, the LFC nerve only appears altered in *Hoxd10* mutants, with no signficant alterations observed in *Hoxa10*$^{-/-}$ animals or in *Hoxa10*$^{-/-}$/*Hoxd10*$^{-/-}$ double-mutant animals. The LFC nerve appears longer in *Hoxd10* mutants. The LFC nerve is entirely sensory, in contrast to the tibial and sciatic nerves which carry mixed sensory and motor fibers. Changes in the LFC may therefore reflect the specific sensitivity of sensory neurons to loss of *Hoxd10* activity or the differential sensitivity of hindlimb nerves to loss of *Hox* gene activity.

Our observations suggest that several hindlimb components are affected by mutations in *Hoxa10* and *Hoxd10*. *Hoxa10* and *Hoxd10* appear to independently regulate aspects of axial and appendicular skeletal patterning, but are likely to interact to regulate the development of hindlimb peripheral innervation. Changes in these elements are likely to contribute to the altered locomotor behavior observed in double-mutant animals.

ACKNOWLEDGMENTS

We thank Mario Capecchi and Jacques Delort for providing *Hoxa10*$^{-/-}$ mice. We thank Andre Der-Avakian for assistance with the initial behavioral and skeletal analysis of *Hoxa10*$^{-/-}$/*Hoxd10*$^{-/-}$ mice, Cecile C. de la Cruz for assistance with whole-mount immunohistochemistry, and Carol Gray and Donna Crandall for figure preparation. The 2H3 hybridoma supernatant was obtained from the Developmental Studies Hybridoma Bank under Contract N01-HD-6-2915 from the NICHD. These studies were funded by NICHD R03HD35843 and by a UCLA Frontiers of Science Faculty Research Award to E.M.C.

REFERENCES

Benson, G. V., Nguyen, T.-H. E., and Maas, R. L. (1995). The expression pattern of the murine *Hoxa-10* gene and the sequence recognition of its homeodomain reveal specific properties of *Abdominal B*-like genes. *Mol. Cell. Biol.* **15,** 1591–1601.

Bürglin, T. R. (1994). A comprehensive classification of homeobox genes. In "Guidebook to the Homeobox Genes" (D. Duboule, Ed.), pp. 27–71. Oxford Univ. Press, London.

Carpenter, E. M., Goddard, J. M., Davis, A. P., Nguyen, T. P., and Capecchi, M. R. (1997). Targeted disruption of *Hoxd-10* affects mouse hindlimb development. *Development* **124,** 4505–4514.

Davis, A. P., and Capecchi, M. R. (1994). Axial homeosis and appendicular skeleton defects in mice with a targeted disruption of *hoxd-11*. *Development* **120,** 2187–2198.

Davis, A. P., and Capecchi, M. R. (1996). A mutational analysis of the 5′ *HoxD* genes: Dissection of genetic interactions during limb development in the mouse. *Development* **122,** 1175–1185.

Davis, A. P., Witte, D. P., Hsieh-Li, H. M., Potter, S. S., and Capecchi, M. R. (1995). Absence of radius and ulna in mice lacking *hoxa-11* and *hoxd-11*. *Nature* **375,** 791–795.

de la Cruz, C. C., Der-Avakian, A., Spyropoulos, D., Tieu, D. D., and Carpenter, E. M. (1999). Targeted disruption of *Hoxd9* and *Hoxd10* alters locomotor behavior, vertebral identity, and peripheral nervous system development. *Dev. Biol.* **216,** 595–610.

Dollé, P., and Duboule, D. (1989). Two gene members of the murine HOX-5 complex show regional and cell-type specific expression in developing limbs and gonads. *EMBO J.* **8,** 1505–1515.

Dollé, P., Izpisúa-Belmonte, J.-C., Falkenstein, H., Renucci, A., and Duboule, D. (1989). Coordinate expression of the murine *Hox-5* complex homeobox-containing genes during limb pattern formation. *Nature* **342,** 767–772.

Edelman, G. M., and Jones, F. S. (1995). Developmental control of N-CAM expression by *Hox* and *Pax* gene products. *Phil. Trans. R. Soc. London B* **349,** 305–312.

Edelman, G. M., and Jones, F. S. (1998). Gene regulation of cell adhesion: A key step in neural morphogenesis. *Brain Res. Rev.* **26,** 337–352.

Favier, B., Le Meur, M., Chambon, P., and Dollé, P. (1995). Axial skeleton homeosis and forelimb malformations in *Hoxd-11* mutant mice. *Proc. Natl. Acad. Sci. USA* **92,** 310–314.

Favier, B., Rijli, F. M., Fromental-Ramain, C., Fraulob, V., Chambon, P., and Dollé, P. (1996). Functional cooperation between the non-paralogous genes *Hoxa-10* and *Hoxd-11* in the developing forelimb and axial skeleton. *Development* **122,** 449–460.

Fromental-Ramain, C., Warot, X., Lakkaraju, S., Favier, B., Haack, H., Birling, C., Dierich, A., Dollé, P., and Chambon, P. (1996a). Specific and redundant functions of the paralogous *Hoxa-9* and *Hoxd-9* genes in forelimb and axial skeleton patterning. *Development* **122,** 461–472.

Fromental-Ramain, C., Warot, X., Messadecq, N., LeMeur, M., Dollé, P., and Chambon, P. (1996b). *Hoxa-13* and *Hoxd-13* play a crucial role in the patterning of the limb autopod. *Development* **122,** 2997–3011.

Gaunt, S. J., Krumlauf, R., and Duboule, D. (1989). Mouse homeogenes within a subfamily, *Hox*-1.4, -2.6 and -5.1, display similar anteroposterior domains of expression in the embryo, but show stage- and tissue-dependent differences in their regulation. *Development* **107,** 131–141.

Goto, J., Miyabayashi, T., Wakamatsu, Y., Takahashi, N., and Muramatsu, M. (1993). Organization and expression of mouse *Hox3* cluster genes. *Mol. Gen. Genet.* **239,** 41–48.

Hall, B. K., and Miyake, T. (2000). All for one and one for all: Condensations and the initiation of skeletal development. *BioEssays* **22,** 138–147.

Izpisúa-Belmonte, J.-C., Falkenstein, H., Dollé, P., Renucci, A., and Duboule, D. (1991). Murine genes related to the *Drosophila AbdB* homeotic gene are sequentially expressed during develoment of the posterior part of the body. *EMBO J.* **10,** 2279–2289.

Kaufman, M. H., and Bard, J. B. L., (1999). "The Anatomical Basis of Mouse Development." Academic Press, San Diego.

Lance-Jones, C. (1979). The morphogenesis of the thigh of the mouse with special reference to tetrapod muscle homologies. *J. Morphol.* **162,** 275–310.

Lance-Jones, C. (1982). Motoneuron cell death in the developing lumbar spinal cord of the mouse. *Dev. Brain Res.* **4,** 473–479.

Peterson, R. L., Papenbrock, T., Davda, M. M., and Awgulewitsch, A. (1994). The murine *Hoxc* cluster contains five neighboring *AbdB*-related *Hox* genes that show unique spatially coordinated expression in posterior embryonic subregions. *Mech. Dev.* **47,** 253–260.

Renucci, A., Zappavigna, V., Zàkàny, J., Izpisúa-Belmonte, J.-C., Bürki, K., and Duboule, D. (1992). Comparison of mouse and human HOX-4 complexes defines conserved sequences involved in the regulation of *Hox-4.4. EMBO J.* **11,** 1459–1468.

Rijli, F. M., and Chambon, P. (1997). Genetic interactions of *Hox* genes in limb development: Learning from compound mutants. *Curr. Opin. Genet. Dev.* **7,** 481–487.

Rijli, F. M., Matyas, R., Pellegrini, M., Dierich, A., Gruss, P., Dollé, P., and Chambon, P. (1995). Cryptorchidism and homeotic transformations of spinal nerves and vertebrae in *Hoxa-10* mutant mice. *Proc. Natl. Acad. Sci USA* **92,** 8185–8189.

Satokata, I., Bensen, G., and Maas, R., (1995). Sexually dimorphic sterility phenotypes in *Hoxa10*-deficient mice. *Nature* **374,** 460–463.

Small, K. M., and Potter, S. S. (1993). Homeotic transformations and limb defects in *Hox A11* mutant mice. *Genes Dev.* **7,** 2318–2328.

Suemori, H., and Noguchi, S. (2000). *Hox C* cluster genes are dispensible for overall body plan of mouse embryonic development. *Dev. Biol.* **220,** 333–342.

Takei, K., Chan, T. A., Wang, F.-S., Deng, H., Rutishauser, U., and Jay, D. G. (1999). The neural cell adhesion molecules L1 and NCAM-180 act in different steps of neurite outgrowth. *J. Neurosci.* **19,** 9469–9479.

Tang, J., Rutishauser, U., and Landmesser, L. (1994). Polysialic acid regulates growth cone behavior duing sorting of motor axons in the plexus region. *Neuron* **13,** 405–414.

Yokouchi, Y., Sasaki, H., and Kuroiwa, A. (1991). Homeobox gene expression correlated with the bifurcation process of limb cartilage development. *Nature* **353,** 443–445.

Received for publication July 20, 2000
Revised November 24, 2000
Accepted November 27, 2000
Published online January 26, 2001